

Influence of spatial dispersion in metals on the optical response of deeply subwavelength slit arraysMathieu Dechaux,^{1,2} Paul-Henri Tichit,^{1,2} Cristian Ciraci,³ Jessica Benedicto,^{1,2} Rémi Pollès,^{1,2} Emmanuel Centeno,^{1,2} David R. Smith,⁴ and Antoine Moreau^{1,2,4}¹*Clermont Université, Université Blaise Pascal, Institut Pascal, BP 10448, F-63000 Clermont-Ferrand, France*²*CNRS, UMR 6602, IP, F-63171 Aubière, France*³*Instituto Italiano di Tecnologia (IIT), Center for Biomolecular Nanotechnologies, Via Barsanti, I-73010 Arnesano, Italy*⁴*Center for Metamaterials and Integrated Plasmonics, Duke University, Durham, North Carolina 27708, USA*

(Received 23 January 2015; revised manuscript received 15 December 2015; published 13 January 2016)

In the framework of the hydrodynamic model describing the response of electrons in a metal, we show that arrays of very narrow and shallow metallic slits have an optical response that is influenced by the spatial dispersion in metals arising from the repulsive interaction between electrons. As a simple Fabry-Perot model is not accurate enough to describe the structure's behavior, we propose considering the slits as generalized cavities with two modes, one being propagative and the other evanescent. This very general model allows us to conclude that the impact of spatial dispersion on the propagative mode is the key factor explaining why the whole structure is sensitive to spatial dispersion. As the fabrication of such structures with relatively large gaps compared to previous experiments is within our reach, this work paves the way for future much needed experiments on nonlocality.

DOI: [10.1103/PhysRevB.93.045413](https://doi.org/10.1103/PhysRevB.93.045413)**I. INTRODUCTION**

Drude's model [1] has proven highly accurate throughout the twentieth century in describing the optical response of metals, despite extensive studies in the 1970s and 1980s to find its limits [2,3]. Recent experiments have however shown that the behavior of resonances in subnanometer-sized gaps cannot be explained with Drude's model alone [4,5], making it necessary to take into account the repulsion between electrons inside the metal in the framework of a hydrodynamic model [6–8]. In that case, the metallic response is spatially dispersive and since it cannot be reduced to a single permittivity depending on the frequency alone, it is often said to be nonlocal. Further experiments would however be welcome because of the subnanometer dimensions of the considered gaps [9,10].

In the present work, we explain why the nonlocal response of metals can be expected to have an impact on deeply subwavelength metallic gratings, a structure that has been extensively studied in the past decade for its extraordinary transmission [11,12] and absorption [13–16]. We underline that these effects will be clear for grooves that are as large as a few nanometers and that the fabrication of such still very narrow slits seems totally within our reach [15–17].

In the first part of this article, we will focus on the physical analysis of the absorption by the metallic slits array when spatial dispersion is neglected. It is now well accepted that the extraordinary optical transmission of slit arrays is due to the excitation of cavity resonances inside the slits [11,18], even if nonresonant mechanisms allow for a high transmission for very thin structures [19]. The only guided mode propagating in the slits in p polarization has actually no cutoff and can propagate whatever the slit width, with a wave vector k_z close to k_0 , the wave vector in vacuum in most cases. This is why, as is usual for cavities, the thickness of the grating is roughly half the wavelength in vacuum for the fundamental resonance [20], except for exotic cases [21]. The same mechanism explains the absorption by subwavelength grooves, the difference being

that, since the cavity is now closed on one end (see Fig. 1), the depth of the grooves is only a quarter of the wavelength in vacuum [14]. In all cases, an extraordinarily strong funneling effect explains the way the energy is literally sucked up into the slits [14,19].

As long as the metal can be considered as almost perfect (in the IR [12,14] or THz [22] or even microwave [23] range) or when the slit is larger than 50 nm in the optical range, the above physical picture is fully accurate. However, below that 50 nm threshold for the slit width in the optical range, the guided mode is more localized in the metal than in the slits because the skin depth δ is typically around 25 nm for noble metals. The mode then experiences what can be called a plasmonic drag: as the width of the gap decreases, it becomes slower and slower, its group velocity goes to zero, and its wave vector k_z diverges [24]. Its effective wavelength, defined as $\lambda_{\text{eff}} = 2\pi/k_z$, thus becomes very small. The depth of the cavity being actually proportional to this effective wavelength [25], the thickness of the grating can be made extremely small and the slits will still constitute a resonator [13]. This is the regime we are interested in, because it is one of the rare structures in which a plasmonic guided mode with a very high wave vector can be excited [7]. We show however that the physics of these resonators is slightly more complicated than previously thought [13]: the slits are so shallow that the guided mode is not the only channel for light to reach the bottom of the structure. A one-mode model [11,18] is thus not sufficient to describe the cavity accurately. We give here a generalized Fabry-Perot formula to better predict the behavior of the resonances.

In the second part, we take into account spatial dispersion in the framework of the hydrodynamic model with realistic parameters [7,26], and show that the response of the structure is influenced by nonlocality. Moreover, using the generalized Fabry-Perot formula, we show that the influence of nonlocality on the wave vector of the guided mode explains almost totally why the structure is so sensitive to spatial dispersion in metals, completing the physical picture.

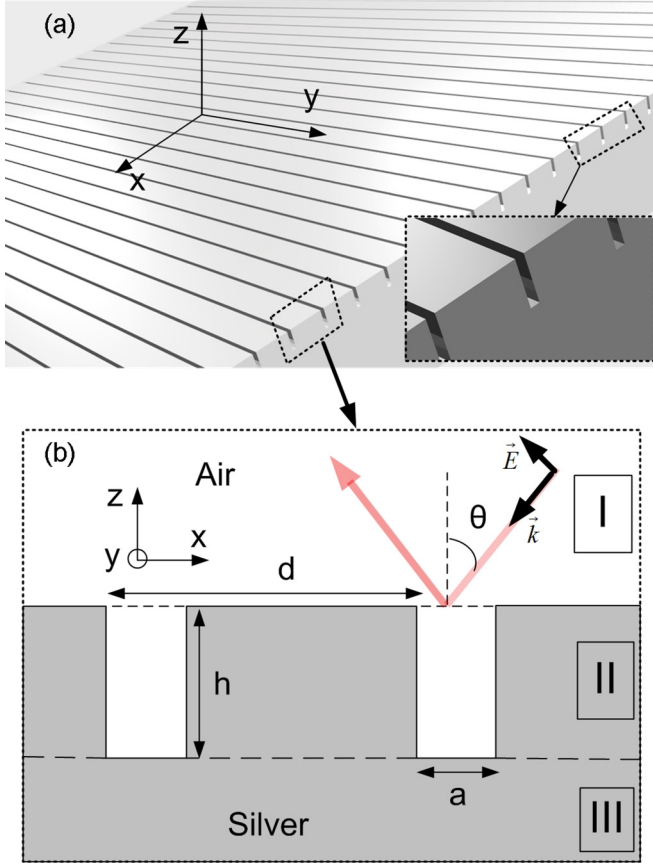


FIG. 1. Representation of the grooves carved in metal, illuminated from above by a TM-polarized plane wave. We distinguish three different layers, layer II being the layer containing the slits.

II. GENERALIZED CAVITY MODEL

The structure considered here [13,15,16] is presented in Fig. 1. It is an infinite array of deeply subwavelength grooves of width a ranging 2 to 5 nm and depth h , from 15 to 30 nm typically. The period d is ranging from 30 to 50 nm in the present study. Since the structure is periodic with a period of the order of twice the skin depth, the slits must be considered as coupled, and the modes propagating in the slits can be found for normal incidence by solving the classical dispersion relation for metallo-dielectric structures [13]

$$\cosh(\kappa a) \cosh[\kappa_i(d-a)] + \frac{1}{2} \left[\frac{\kappa_i}{\epsilon\kappa} - \frac{\epsilon\kappa}{\kappa_i} \right] \sinh(\kappa a) \sinh[\kappa_i(d-a)] - 1 = 0, \quad (1)$$

where $\kappa_i^2 = k_n^2 - \epsilon k_0^2$ and $\kappa^2 = k_n^2 - k_0^2$, ϵ being the permittivity of the metal and $k_0 = 2\pi/\lambda$.

The different modes are indexed by n and characterized by a propagation constant k_z along the z axis, and a magnetic field profile $H_y^n(x)$. The magnetic field in layer II can thus be written as a sum of modes propagating upward or downward:

$$H_y(x, z) = \sum_n H_y^n(x) [A_n e^{-i k_n z} + B_n e^{+i k_n z}] e^{-i\omega t}. \quad (2)$$

As expected, there is only one propagating Bloch mode (presenting a propagation constant k_1 with a dominant real

part). All the other modes are evanescent and thus attenuated in the z direction, with essentially imaginary propagation constants k_n . The propagative mode is reflected back and forth in the slits, thus producing the resonance. The actual reflection coefficients (r_1 for the interface between the grating and air, r_1^b for the bottom of the grooves) can be computed using rigorous coupled-wave analysis (RCWA) [27,28], as is quite common for metallic gratings [18,21]. We underline that the computation of the reflection coefficients requires the computation of many evanescent modes. One could expect, from the vast literature on the subject, that the reflection coefficient of the whole structure can simply be written using a Fabry-Perot formula:

$$r = r_0 + \frac{r_1 t_{01} t_{10} e^{2ik_1 h}}{1 - r_1 r_1^b e^{2ik_1 h}}, \quad (3)$$

where t_{01} is the transmission coefficient from the incoming plane wave to the propagating mode in the slits and t_{10} the transmission coefficient from the mode in the slits to the outgoing plane wave, which are computed using RCWA. While such an approach has proved extremely accurate in the past for the extraordinary optical transmission (EOT) [11,18,21,29], here, quite unexpectedly, it fails to predict the position of the resonance given by local RCWA full simulations (see Fig. 2).

The assumption underlying (3) is that only the propagative mode is able to reach the bottom of the grooves. However, because the depth of the grating is smaller than the skin depth, not all the evanescent modes are attenuated enough to be neglected. To be more precise, one mode in particular, although it is not propagative in the z direction, presents an attenuation constant that is so low that it is still significantly strong at the bottom of the slits.

The profile of this mode is shown Fig. 2 and it is relatively flat. This mode is thus very close to the attenuated wave that is excited in the metal when a plane wave is reflected by a metallic screen. Moreover, each reflection of the propagating mode at the top or at the bottom of the grooves generates this mode too, so that it fully participates to the resonance. We propose here a very general two-mode approach to model the reflection coefficient of the structure.

In this framework, we call A_1 and B_1 (resp. A_2 and B_2) the amplitude of the propagating (resp. evanescent) mode traveling (resp. attenuating) downwards or upwards (see Fig. 2). The reflection coefficient of the whole structure can then be written as the result of the reflection on the metallic plane plus the light that comes from the two modes inside the grating layer:

$$r = r_0 + t_{10} B_1 + t_{20} B_2. \quad (4)$$

The downward amplitudes can be written as a result of the direct excitation by the incoming plane wave, in addition to the reflection of the modes inside the slits,

$$A_1 = t_{01} + r_1 B_1 + r_{21} B_2,$$

$$A_2 = t_{02} + r_2 B_2 + r_{12} B_1,$$

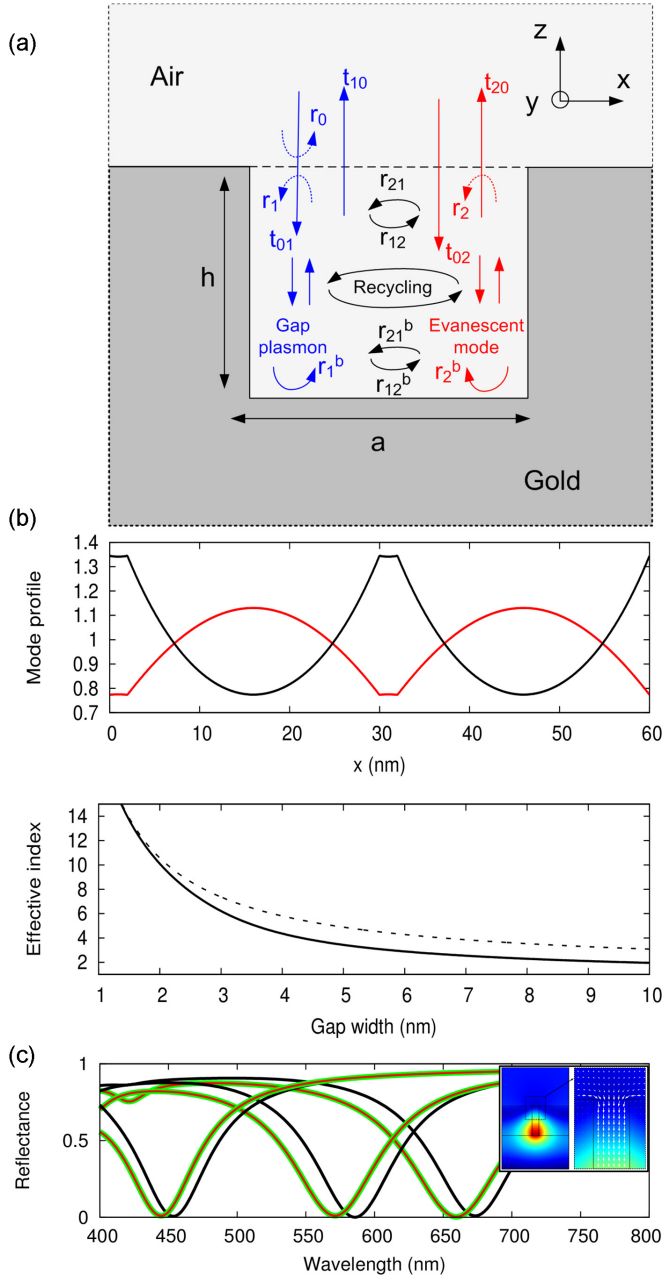


FIG. 2. (a) Representation of the generalized cavity model with the different reflection coefficients. (b) Top: Profile of the propagating mode (black curve) and the first evanescent mode (red curve). Bottom: Diverging effective index of the propagating mode as a function of the gap width (solid line) and the mode guided in a single isolated slit, the gap-plasmon polariton (dotted line). (c) Reflection coefficient of the whole structure, considering only the fundamental Bloch mode (black curve), a 2-mode model (red curve), and a complete simulation (green curve) for different groove depths (left: 7 nm; center: 3 nm; right: 2 nm). Inset: Simulation with COMSOL Multiphysics of the magnetic field and the Poynting vector at the entrance of the slits.

and the equivalent is obtained at the bottom of the grooves for the upward amplitudes,

$$\begin{aligned} B_1 e^{-ik_1 h} &= r_1^b A_1 e^{ik_1 h} + r_{21}^b B_2 e^{ik_2 h}, \\ B_2 e^{-ik_2 h} &= r_2^b A_1 e^{ik_1 h} + r_{12}^b A_2 e^{ik_2 h}. \end{aligned}$$

This forces us to introduce all the above new reflection and coupling coefficients, which can be computed using RCWA. This approach is inspired by mode recycling in photonic crystal cavities [30], generalized here to (i) a nonsymmetrical plasmonic cavity and (ii) the case where the evanescent mode can be directly excited by the incident wave.

We first use the relation above to eliminate B_2 from the whole system, yielding

$$\begin{aligned} r &= r_0 + t_{10} B_1 + t_{20} (r_2^b A_2 e^{2ik_2 h} + r_{12}^b A_1 e^{i(k_1+k_2)h}), \\ A_1 &= t_{01} + r_1 B_1 + r_{21} (r_2^b A_2 e^{2ik_2 h} + r_{12}^b A_1 e^{i(k_1+k_2)h}), \\ A_2 &= t_{02} + r_1 (r_2^b A_2 e^{2ik_2 h} + r_{12}^b A_1 e^{i(k_1+k_2)h}) + r_{12} B_1, \\ B_1 &= r_1^b A_1 e^{2ik_1 h} + r_{21}^b A_2 e^{i(k_1+k_2)h}. \end{aligned}$$

We finally get from these equations an expression for A_2 ,

$$A_2 = t'_{02} + c A_1 + r'_{12} B_1,$$

where

$$\begin{aligned} t'_{02} &= \frac{t_{02}}{1 - r_2 r_2^b e^{2ik_2 h}}, \\ c &= \frac{r_2 r_{12}^b e^{i(k_2+\gamma_1)h}}{1 - r_2 r_2^b e^{2ik_2 h}}, \\ r'_{12} &= \frac{r_{12}}{1 - r_2 r_2^b e^{2ik_2 h}}. \end{aligned}$$

We can thus replace A_2 in the above equations, to yield

$$\begin{aligned} r &= r'_0 + t'_{10} B_1 + \alpha A_1, \\ A_1 &= t_{01} + r_1 B_1 + r_{21} [r_2^b (t'_{02} + c A_1 + r'_{12} B_1) e^{2ik_2 h} + r_{12}^b A_1 e^{i(k_1+k_2)h}], \\ B_1 &= r_1^b A_1 e^{2ik_1 h} + r_{21}^b (t'_{02} + c A_1 + r'_{12} B_1) e^{i(k_1+k_2)h}, \end{aligned}$$

where

$$\begin{aligned} r'_0 &= r_0 + t_{20} r_2^b t'_{02} e^{2ik_2 h}, \\ t'_{10} &= t_{10} + t_{20} r_2^b r'_{12} e^{2ik_2 h}, \\ \alpha &= t_{20} r_{12}^b e^{i(k_1+k_2)h} + t_{20} r_2^b c e^{2ik_2 h}. \end{aligned}$$

And finally, the system reduces to

$$\begin{aligned} r &= r'_0 + t'_{10} B_1 + \alpha A_1, \\ A_1 &= r'_1 B_1 + t'_{01}, \\ B_1 &= r_1^b A_1 e^{2ik_1 h} + t''_{02}, \end{aligned}$$

where

$$\begin{aligned} r'_1 &= \frac{r_2^b r_{21} r'_{12} e^{2ik_2 h}}{1 - r_{21} r_{12}^b e^{i(k_1+k_2)h}}, \\ t'_{01} &= t_{01} + t'_{02} r_{21} r_2^b e^{2ik_2 h}, \\ r_1^b &= \frac{r_1^b r_{21}^b c e^{i(k_2-\gamma_1)h}}{1 - r_{21}^b r_{12}^b e^{i(k_2-k_1)h}}, \\ t''_{02} &= \frac{t'_{02} r_{21}^b e^{i(k_2+\gamma_1)h}}{1 - r_{21}^b r_{12}^b e^{i(k_2+k_1)h}}. \end{aligned}$$

It is not obvious yet that these equations can be used to yield a generalized Fabry-Perot formula, because two terms have

appeared that do not exist in the classical one-mode model. More precisely, to retrieve the exact same equations, t''_{02} and α would have to vanish. This is usually the case in photonic crystals—but physically here, the evanescent mode is directly and efficiently excited by the incoming wave so that t''_{02} is not negligible.

We now replace A_1 with its expression in the reflection coefficient's formula, to yield

$$\begin{aligned} r &= r''_0 + t''_{10} B_1, \\ B_1 &= r'_1 e^{2ik_1 h} A_1 e^{2ik_1 h} + t''_{02}, \\ A_1 &= r'_1 B_1 + t'_{01}, \end{aligned}$$

where new effective coefficients are introduced:

$$r''_0 = r'_0 + \alpha t'_{01}, \quad (5)$$

$$t''_{10} = t'_{10} + \alpha r'_1. \quad (6)$$

Finally, A_1 can be written

$$A_1 = \frac{t'_{01} + t''_{02} r'_1}{1 - r'_1 r'_1 e^{2ik_1 h}}, \quad (7)$$

and the reflection coefficient, by eliminating B_1 , gives

$$r = r''_0 + t''_{10} r'_1 e^{2ik_1 h} A_1 e^{2ik_1 h} + t''_{02}, \quad (8)$$

leading to the desired result

$$r = r''_0 + t''_{10} t''_{02} + \frac{r'_1 e^{2ik_1 h} t''_{10} (t'_{10} + t''_{02} r'_1)}{1 - r'_1 r'_1 e^{2ik_1 h}}. \quad (9)$$

If we call

$$r_{\text{eff}} = r''_0 + t''_{10} t''_{02}, \quad (10)$$

$$t_{\text{eff}} = t''_{10} (t'_{10} + t''_{02} r'_1), \quad (11)$$

then the reflection coefficient can be put under a form similar to the Fabry-Perot formula,

$$r = r_{\text{eff}} + \frac{t_{\text{eff}} r'_1 e^{2ik_1 h}}{1 - r'_1 r'_1 e^{2ik_1 h}}. \quad (12)$$

This formula can be considered as a generalized Fabry-Perot formula. The agreement between this formula and a full RCWA simulation [see Fig. 2(c)], which can be considered as a multimode model, is excellent. The two modes are thus the only ones that are responsible for the resonance. More precisely, the propagating mode is responsible for the resonance and the evanescent mode is responsible for a shift of this resonance compared to the one-mode model.

The effective reflection coefficients are easy to compute, once the real coefficients are extracted from the scattering matrices of the interfaces between the different space regions [21]. The resonance condition now reads

$$\arg(r'_1) + \arg(r'_1 e^{2ik_1 h}) + 2\text{Re}(k_1)h = 2m\pi, \quad (13)$$

where m is a relative integer. Figure 3 shows the phase of the effective reflection coefficients, compared to the phase of the real reflection coefficients. There is essentially a shift of the phase of r'_1 compared to the one of r_1 . This totally explains why, compared to the one-mode model prediction, the resonance is

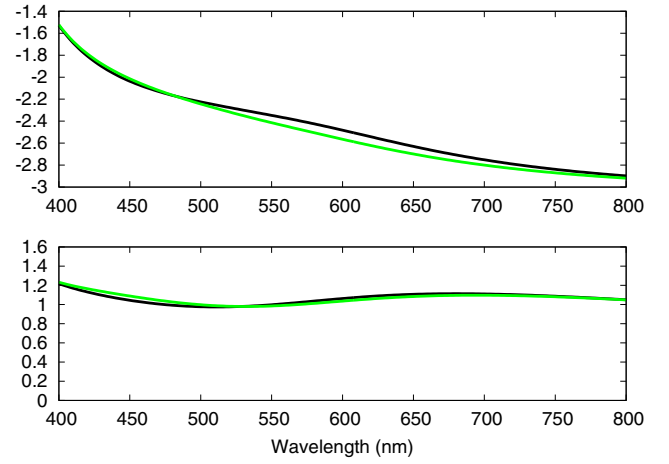


FIG. 3. Phase of the reflection coefficients. Top: Phase of r_1 and r'_1 (black and green curves, respectively). Bottom: Phase of r''_1 and r''_1' (black and green lines, respectively).

shifted since the shift in the phase has a direct impact on the resonance condition. The fact that the slope of the phase is not changed means that there is almost no impact on the quality factor of the resonance, so that the only impact of the second mode on the resonance is to shift it without changing its width.

III. IMPACT OF SPATIAL DISPERSION

Deeply subwavelength gratings are very interesting because the absorbing resonance is the sign that a guided mode with a very high wave vector has been efficiently excited in the structure. Such modes are likely to be influenced by the repulsion between electrons [7] because their effective wavelength is so small that it approaches the mean-free path of electrons in the metal [31], which is the relevant scale for nonlocality. That is the reason why the spatial dispersion is expected to have an impact on the slit array's response.

We use here the hydrodynamic model [7,8] to take the intrinsic nonlocality of the metallic response into account. The currents \mathbf{J} corresponding to the movement of the free electrons trapped in the metal can be taken into account as an effective polarization \mathbf{P}_f defined by $\dot{\mathbf{P}}_f = \mathbf{J}$. The electron gas can be considered as a fluid [6], leading to the following linearized equation

$$-\beta^2 \nabla(\nabla \cdot \mathbf{P}_f) + \ddot{\mathbf{P}}_f + \gamma \dot{\mathbf{P}}_f = \epsilon_0 \omega_p^2 \mathbf{E}, \quad (14)$$

where γ is the damping factor, ω_p the plasma frequency, and $\beta \simeq 1.35 \times 10^6$ m/s. All these parameters (except β), as well as the dispersive susceptibility χ_b due to interband transitions, are taken from careful fits of the available experimental data using a Drude and Brendel-Bormann model [32]. This allows us to clearly distinguish between the response of the jellium and the response of the background, which we assume is local. Maxwell's equations then reduce to [7]

$$\begin{aligned} \nabla \times \mathbf{E} &= i\omega\mu_0 \mathbf{H}, \\ \nabla \times \mathbf{H} &= -i\omega\epsilon_0(1 + \chi_b)\mathbf{E} + \mathbf{P}_f, \end{aligned}$$

where, thanks to (14), the polarization can be written as

$$\mathbf{P}_f = \frac{\epsilon_0 \omega_p^2}{\omega^2 + i\gamma\omega} \left[\mathbf{E} - (1 + \chi_b) \frac{\beta^2}{\omega_p^2} \nabla(\nabla \cdot \mathbf{E}) \right]. \quad (15)$$

The resolution of such equations in a multilayered structure requires the introduction of an additional boundary condition (ABC). The most obvious ABC is in that case to consider that no electrons are allowed to get out of the metal [25], which means $\mathbf{J} \cdot \mathbf{n} = \mathbf{P}_f \cdot \mathbf{n} = 0$, where \mathbf{n} is the normal to the interface—and it turns out to be one of the most conservative ABCs, so that nonlocal effects are not likely to be overestimated [7].

In this framework the dispersion relation giving the propagation constant of the modes is modified [26] and becomes

$$\begin{aligned} 1 - \left[\frac{\epsilon\Omega \sinh(\kappa_t e)}{k_z \sinh(\kappa_l e)} \right] \\ = \cosh(\kappa a) \cosh(\kappa_t e) \\ + \frac{1}{2} \left[\frac{\kappa_t}{\epsilon\kappa a} - \frac{\epsilon\kappa a}{1 - \kappa_t} + \Omega^2 \left(\frac{\epsilon}{\beta\kappa_t e} \right) \right] \sinh(\kappa a) \sinh(\kappa_t e) \\ + \frac{\Omega}{\sinh(\kappa_l e)} \left\{ \frac{\sinh(\kappa a)}{\beta} \left[1 - \cosh(\kappa_t e) \cosh(\kappa_l e) \right] \right. \\ \left. - \frac{\epsilon \sinh(\kappa_t e)}{\kappa_t} \cosh(\kappa a) \cosh(\kappa_l e) \right\}, \quad (16) \end{aligned}$$

where $e = d - a$, $\Omega = \frac{k_z^2}{\kappa_l} \left(\frac{1}{\epsilon} - \frac{1}{1 + \chi_b} \right)$, $\kappa_l^2 = k_z^2 + \left(\frac{\omega_p^2}{\beta^2} \right) \left(\frac{1}{\chi_f} + \frac{1}{1 + \chi_b} \right)$, $\kappa_t^2 = k_z^2 - \epsilon k_0^2$, and $\kappa^2 = k_z^2 - k_0^2$. This allows us to consider the impact of nonlocality on the propagation constants of the two modes that are involved in the resonance of the structure—both the propagating and the least evanescent of the remaining modes, as shown Fig. 4. The figure actually shows that the propagating mode is significantly more sensitive to

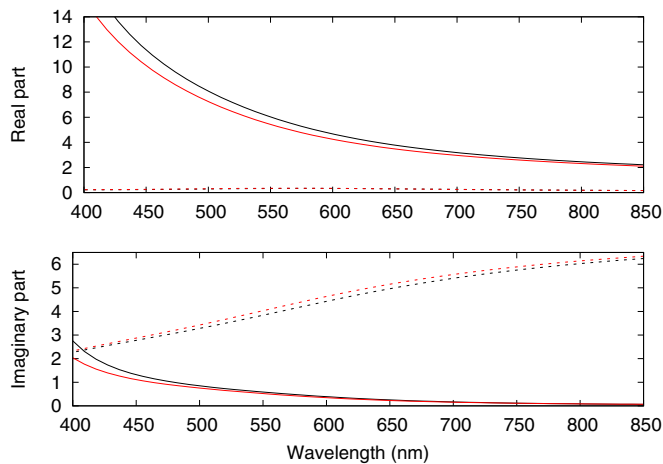


FIG. 4. Impact of nonlocality on the effective index (phase index) of the propagating mode (solid line) and on the evanescent mode (dashed line). The real (top) and imaginary (bottom) parts of the propagation constant are shown for a purely local approach (in black) and in the framework of the hydrodynamic model (red).

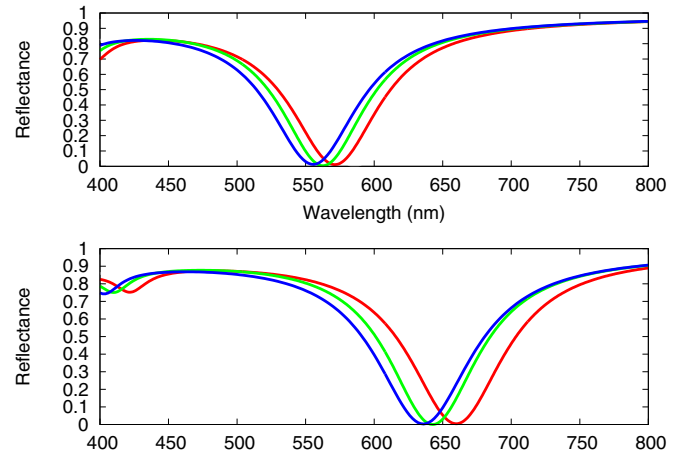


FIG. 5. Reflection coefficient computed using COMSOL (fully nonlocal calculation, blue curves), using a local 2-mode model (red curves) and using a nonlocal version of the 2-mode model (green curves) for 3 nm wide grooves (top) and 2 nm wide grooves (bottom).

nonlocality because of its large wave vector k_1 . A high wave vector actually means a large value for Ω and thus a noticeable effect on the dispersion relation.

In order to assess the impact of nonlocality on the whole structure, we have used COMSOL simulations, as a full non-local modal method is still beyond our reach. As expected, the resonance is blueshifted compared to a local calculation [from 15 nm for 3 nm wide slits, see Fig. 5(b), to 24 nm for 2 nm wide slits, see Fig. 5(a)]. Interestingly, using a two-mode model but changing only the propagation constant k_1 of the fundamental mode as computed using the nonlocal dispersion relation (16) allows us to account for most of the shift (see Fig. 5). This demonstrates that the major reason why the whole structure is sensitive to the spatially dispersive response of the metal is that nonlocality has an impact on the wave vector of the single mode propagating in the slits. Its wave vector is actually not as high as predicted by the local theory, thus leading to a blueshift of the resonance.

IV. CONCLUSION

The mode propagating in a single extremely thin slit is often called a gap-plasmon polariton, to distinguish it from the surface plasmon polariton. The propagating mode considered here is of course closely related and is submitted to the same physical effect: the presence of the metal makes the mode slow, with a very large wave vector. This allows to understand (i) that deeply subwavelength structures, sometimes smaller than the skin depth, can still be considered as cavities and (ii) why, as we have shown here, the smallest resonators are likely to be influenced by spatial dispersion in metals. This class of resonators is called gap-plasmon resonators and it has recently been demonstrated experimentally that these resonators could constitute extraordinarily efficient concentrators and absorbers [15,16,33–35] and produce totally unprecedented Purcell enhancements [36,37]. Theoretical studies show that they have a lot of potential as scatterers for light extraction too [38,39]. We are thus confident that the very general theoretical

tools we have introduced here can be useful to study these structures and help design them in the future, as they reach sizes that are well below the size of conventional cavity resonators.

ACKNOWLEDGMENT

This work has been supported by the Agence Nationale de la Recherche (ANR), Project No. ANR-13-JS10-0003.

-
- [1] P. Drude, *Ann. Phys.* **306**, 566 (1900).
- [2] A. D. Boardman, *Electromagnetic Surface Modes* (Wiley, Chichester, New York, 1982).
- [3] F. Frostmann and R. R. Gerhardt, *Metal Optics Near the Plasma Frequency* (Springer-Verlag, Berlin, Heidelberg, 1986).
- [4] C. Ciraci, R. Hill, J. Mock, Y. Urzhumov, A. Fernández-Domínguez, S. Maier, J. Pendry, A. Chilkoti, and D. Smith, *Science* **337**, 1072 (2012).
- [5] C. Ciraci, X. Chen, J. J. Mock, F. McGuire, X. Liu, S.-H. Oh, and D. R. Smith, *Appl. Phys. Lett.* **104**, 023109 (2014).
- [6] N. Crouseilles, P. A. Hervieux, and G. Manfredi, *Phys. Rev. B* **78**, 155412 (2008).
- [7] A. Moreau, C. Ciraci, and D. R. Smith, *Phys. Rev. B* **87**, 045401 (2013).
- [8] C. Ciraci, J. B. Pendry, and D. R. Smith, *ChemPhysChem* **14**, 1109 (2013).
- [9] T. V. Teperik, P. Nordlander, J. Aizpurua, and A. G. Borisov, *Phys. Rev. Lett.* **110**, 263901 (2013).
- [10] G. Hajisalem, Q. Min, R. Gelfand, and R. Gordon, *Opt. Express* **22**, 9604 (2014).
- [11] J. A. Porto, F. J. García-Vidal, and J. B. Pendry, *Phys. Rev. Lett.* **83**, 2845 (1999).
- [12] X.-R. Huang, R.-W. Peng, and R.-H. Fan, *Phys. Rev. Lett.* **105**, 243901 (2010).
- [13] J. LePerchec, P. Quemerais, A. Barbara, and T. Lopez-Rios, *Phys. Rev. Lett.* **100**, 066408 (2008).
- [14] F. Pardo, P. Bouchon, R. Haïdar, and J.-L. Pelouard, *Phys. Rev. Lett.* **107**, 093902 (2011).
- [15] A. Polyakov, H. A. Padmore, X. Liang, S. Dhuey, B. Harteneck, J. P. Schuck, and S. Cabrini, *J. Vac. Sci. Technol. B* **29**, 06FF01 (2011).
- [16] A. Polyakov, K. Thompson, S. Dhuey, D. Olynick, S. Cabrini, P. Schuck, and H. Padmore, *Sci. Rep.* **2**, 933 (2012).
- [17] X. Chen, C. Ciraci, D. R. Smith, and S.-H. Oh, *Nano Lett.* **15**, 107 (2014).
- [18] P. Lalanne, J. Hugonin, S. Astilean, M. Palamaru, and K. Möller, *J. Opt. A: Pure Appl. Opt.* **2**, 48 (2000).
- [19] G. Subramania, S. Foteinopoulou, and I. Brener, *Phys. Rev. Lett.* **107**, 163902 (2011).
- [20] F. Marquier, J.-J. Greffet, S. Collin, F. Pardo, and J. Pelouard, *Opt. Express* **13**, 70 (2005).
- [21] A. Moreau, C. Lafarge, N. Laurent, K. Edee, and G. Granet, *J. Opt. A: Pure Appl. Opt.* **9**, 165 (2007).
- [22] R.-H. Fan, R.-W. Peng, X.-R. Huang, J. Li, Y. Liu, Q. Hu, M. Wang, and X. Zhang, *Adv. Mater.* **24**, 1980 (2012).
- [23] N. Aközbek, N. Mattiucci, D. de Ceglia, R. Trimm, A. Alù, G. D'Aguzzo, M. Vincenti, M. Scalora, and M. Bloemer, *Phys. Rev. B* **85**, 205430 (2012).
- [24] S. I. Bozhevolnyi and T. Søndergaard, *Opt. Express* **15**, 10869 (2007).
- [25] W. Yan, M. Wubs, and N. A. Mortensen, *Phys. Rev. B* **86**, 205429 (2012).
- [26] J. Benedicto, R. Pollès, C. Ciraci, E. Centeno, D. R. Smith, and A. Moreau, *J. Opt. Soc. Am. A* **32**, 1581 (2015).
- [27] P. Lalanne and G. M. Morris, *J. Opt. Soc. Am. A* **13**, 779 (1996).
- [28] G. Granet and B. Guizal, *J. Opt. Soc. Am. A* **13**, 1019 (1996).
- [29] L. Martín-Moreno, F. J. García-Vidal, H. J. Lezec, K. M. Pellerin, T. Thio, J. B. Pendry, and T. W. Ebbesen, *Phys. Rev. Lett.* **86**, 1114 (2001).
- [30] C. Sauvan, G. Lecamp, P. Lalanne, and J. Hugonin, *Opt. Express* **13**, 245 (2005).
- [31] P.-O. Chapuis, S. Volz, C. Henkel, K. Joulain, and J.-J. Greffet, *Phys. Rev. B* **77**, 035431 (2008).
- [32] A. D. Rakic, A. B. Djurišić, J. M. Elazar, and M. L. Majewski, *Appl. Opt.* **37**, 5271 (1998).
- [33] A. Moreau, C. Ciraci, J. J. Mock, R. T. Hill, Q. Wang, B. J. Wiley, A. Chilkoti, and D. R. Smith, *Nature (London)* **492**, 86 (2012).
- [34] T. Siegfried, Y. Ekinici, O. J. Martin, and H. Sigg, *Nano Lett.* **13**, 5449 (2013).
- [35] D. T. Søndergaard, S. M. Novikov, T. Holmgaard, R. L. Eriksen, J. Beermann, Z. Han, K. Pedersen, and S. I. Bozhevolnyi, *Nat. Commun.* **3**, 969 (2012).
- [36] G. M. Akselrod, C. Argyropoulos, T. B. Hoang, C. Ciraci, C. Fang, J. Huang, D. R. Smith, and M. H. Mikkelsen, *Nat. Photonics* **8**, 835 (2014).
- [37] T. B. Hoang, G. M. Akselrod, C. Argyropoulos, J. Huang, D. R. Smith, and M. H. Mikkelsen, *Nat. Commun.* **6**, 7788 (2015).
- [38] J. Jung, T. Søndergaard, and S. I. Bozhevolnyi, *Phys. Rev. B* **79**, 035401 (2009).
- [39] A. Jouanin, J.-P. Hugonin, M. Besbes, and P. Lalanne, *Appl. Phys. Lett.* **104**, 021119 (2014).